

Electrical and structural characteristics of spray deposited $(\text{ZnO})_X\text{-(CdO)}_{1-X}$ thin films

G. Alarcón-Flores^a, B. Vásquez-Pérez^b, A. Peláez-Rodríguez^a, M. Villa-García^a, S. Carmona-Téllez^a,
J. A. Luna-Guzmán^a, C. Falcony^c, and M. Aguilar-Fruti^s^a

^aCentro de Investigación en Ciencia Aplicada y Tecnología Avanzada del Instituto Politécnico Nacional,
Legaria 694, Col. Irrigación, Del. Miguel Hidalgo, 11500, México D.F., México.

^bUniversidad Autónoma Metropolitana-Azcapotzalco,
Avenida San Pablo Xalpa 180, Reynosa Tamaulipas, Del. Azcapotzalco, 02200 México D.F., México.

^cCentro de Investigación y de Estudios Avanzados del Instituto Politécnico Nacional,
Apartado Postal 14-740, México 07000, D.F., México.

Received 1 February 2013; accepted 18 April 2013

$(\text{ZnO})_X(\text{CdO})_{1-X}$ thin films were deposited on glass substrates at 300°C and 400°C by ultrasonic spray pyrolysis with compositions ranging from CdO to ZnO. The electrical properties were obtained by impedance spectroscopy and Hall Effect measurements. Scanning electron microscopy, energy dispersive spectroscopy, and X-ray diffraction, were used to study the structural characteristics of the films. Ellipsometry, in addition, was used to confirm the structural characteristics. The films as deposited resulted mainly polycrystalline and dense, depending on the substrate temperature and on their relative composition. All the films showed n-type conductivity and the films with intermediate compositions resulted in a mixture of both phases; CdO and ZnO. Hall Effect measurements showed that the highest conductivity of CdO was close to $1 \times 10^3 (\Omega\text{-cm})^{-1}$, the highest value obtained for CdO, without doping. Impedance spectroscopy confirmed the Hall Effect results, showing that the highly conducting character of CdO influenced dramatically the conductivity of the $(\text{ZnO})_X(\text{CdO})_{1-X}$ films. In addition, depending on the substrate temperature and on the relative composition of the films, both, the bulk or grains, as well as the grain boundaries properties limit the conductivity in them.

Keywords: Impedance spectroscopy; transparent conducting oxides (tcos); spray pyrolysis

Películas delgadas de $(\text{ZnO})_X(\text{CdO})_{1-X}$ fueron depositadas sobre sustratos de vidrio a 300°C y 400°C por rocío pirolítico ultrasónico con composiciones entre CdO y ZnO. Las propiedades eléctricas fueron determinadas a través de medidas de espectroscopia de impedancia y Efecto Hall. Microscopia electrónica de barrido, espectroscopia por dispersión de energía y difracción de rayos X fueron utilizadas para determinar las características estructurales de las películas. Elipsometría fue empleada para confirmar las características estructurales. Las películas, tal y como son depositadas resultaron policristalinas y densas, dependiendo de la temperatura del sustrato y de la composición relativa de ellas. Todas las películas mostraron una conductividad de tipo n y las películas con concentraciones intermedias resultaron con una mezcla de ambas fases; CdO y ZnO. Las mediciones de Efecto Hall mostraron que la más alta conductividad de las películas de CdO fue cercano a $1 \times 10^3 (\Omega\text{-cm})^{-1}$, valor más alto obtenido para CdO sin dopante. Las medidas de espectroscopia de impedancia confirmaron los resultados obtenidos por Efecto Hall, y mostraron además que el alto carácter conductor de las películas de CdO influye de manera importante en la conductividad de las películas de $(\text{ZnO})_X(\text{CdO})_{1-X}$. Además, dependiendo de la temperatura del sustrato y de la composición relativa de las películas ambos, los granos (o el bulto), así como las fronteras de grano, limitan la conductividad en ellas.

Descriptores: Espectroscopia de impedancia; óxidos conductores transparentes (TCOs); rocío pirolítico

PACS: 84.37.+q; 73.50-h; 68.55-a

1. Introduction

Transparent conducting oxides (TCO's) have been known and employed technologically for a long time. Some of the applications include portable electronics, displays, flexible electronics, multi-functional windows, solar cells, and transistors. In addition, semiconductors, molecular and polymer organics, ceramics, glass, metal and plastic, have necessitated TCO materials with new performance, processability and morphology [1]. Zinc oxide (ZnO), cadmium oxide (CdO), indium oxide (In_2O_3), tin oxide (SnO_2), and tin doped indium oxide (ITO) belong to the class of conventional TCO materials that have been investigated for the latter types of applications and more [2]. Even though, a lot of work has been done in the conventional TCO's, many basic is-

ues are still under research in them [1]. Not long ago, A. J. Freeman *et al.* proposed some strategies to develop new TCO's [3]. The combination or mixture of two (or more), of them, such as: ZnO and CdO, in order to get a mixed TCO, results interesting because of the individual properties that each one of them possess. ZnO is characterized by a wide direct energy band gap ($E_g \sim 3.3$ eV at 300 K), its best room-temperature electron mobility is ~ 205 cm^2/Vs and carrier concentration about $6.0 \times 10^{16} \text{ cm}^{-3}$, among other interesting properties [4,5]. CdO, on the other hand, is probably the oxide that exhibits the highest conductivity. Its high conductivity results mainly because under usual preparation conditions the compound is oxygen deficient, and has a relatively large concentration of ionized atomic defects, either oxygen vacancies or cadmium interstitials [6]. Its conductivity can

be even increased up to $\sim 7.1 \times 10^3 (\Omega\text{-cm})^{-1}$, the highest value ever reported for CdO film when doped with Sn [7]. However, a serious disadvantage of CdO is the relatively low band gap ($E_g \sim 2.4$ eV) [8]. It has been proposed that the mixing of these oxides could lead to a single film with high electrical conductivity and high optical transmittance in the visible range of the electromagnetic spectrum [9-18]. In addition, the scarceness and low availability in the earth crust of indium (0.1 ppm) has motivated to pursue new TCO's [1], for this reason, any attempt to engineer an alternative or new TCO with properties close to ITO is an issue of great scientific and technological interest. The CdO-ZnO thin film system has already been studied. For example, ZnCdO epilayers have been grown by a radical-source MBE technique with improved crystalline quality [9]. The crystalline quality has also been studied in $\text{Cd}_x\text{Zn}_{1-x}\text{O}$ alloy thin films using a sequential pulsed laser deposition method [10]. The structural and optical properties of $\text{Cd}_x\text{Zn}_{1-x}\text{O}$ ternary alloy thin films have been investigated when deposited by pulsed-laser deposition [11]. The optical properties of $\text{Cd}_x\text{Zn}_{1-x}\text{O}$ thin films, deposited by ultrasonic spray pyrolysis, have also been investigated, as well as its gas-sensing properties [12,13]. The optical and structural properties of $\text{Cd}_x\text{Zn}_{1-x}\text{O}$ thin films have also been studied when deposition is carried out pneumatically by spray pyrolysis by O. Vigil and G. Santana [14,15], as well as the effect of a post-thermal annealing in the films [16]. However, as much as we revised in the literature, the impedance spectroscopy characteristics of the $(\text{ZnO})_x(\text{CdO})_{1-x}$ system had been scarcely reported. So, in this work, $(\text{ZnO})_x(\text{CdO})_{1-x}$ thin films were spray pyrolyzed at 300°C and 400°C and characterized without any post-thermal annealing by impedance spectroscopy. Additional electrical characteristics were got by Hall Effect measurements. Furthermore, some of the structural properties of the films, and the index of refraction are described.

2. Experimental

The $(\text{ZnO})_x(\text{CdO})_{1-x}$ films were prepared with different relative concentrations of cadmium and zinc acetates $[(\text{C}_2\text{H}_3\text{O}_2)_2\text{Cd} \cdot 2\text{H}_2\text{O}$ and $(\text{C}_2\text{H}_3\text{O}_2)_2\text{Zn} \cdot 2\text{H}_2\text{O}$, respectively], but keeping constant the total molarity (0.1 M), in a methanol- H_2O (1:1) solution, using the Ultrasonic Spray Pyrolysis Technique. The films were deposited at 300°C and 400°C on corning glass substrates. The spray pyrolysis deposition system has been described elsewhere [19,20]. It consists of an ultrasonic generator for mist production from a spraying solution. A carrier gas is used to transport the mist on top of the substrate which is placed on a heated surface, in order to achieve the pyrolysis reaction. In this work, a molten tin bath was used as thermal energy source in order to achieve the pyrolysis reaction. The films were deposited during a period of time up to 10 minutes, approximately. Air was used as carrier gas at a flow rate of 10 liters per minute, and two commercial ultrasonic humidifiers, operating at 1.4 MHz and 0.8 MHz, were used for the mist production. The description

of the films is listed in Table I and is as follows: Films A to D, and E to H corresponded to films deposited at 300°C and 400°C, respectively, with A and E, and D and H corresponding to pure CdO and ZnO, respectively. The films as deposited were analyzed by several characterization techniques. A Hall Effect measurements system (van der Pauw, ECOPIA HMS 3000), and a Solartron SI 1260 Impedance/Gain phase analyzer were used to measure the electrical properties of the films, the latter was used in the frequency range of 32 MHz to 0.1 Hz, and applying a 20 mV AC sinusoidal excitation. The impedance measurements were carried out using silver paint coplanar electrodes placed on top of the films' surface [21,22]. The $(\text{ZnO})_x(\text{CdO})_{1-x}$ films with the silver paint electrodes were heated at $\sim 200^\circ\text{C}$ for 1 hour to remove any organic residue and to achieve a better electric contact. The structural characteristics were determined by X-ray diffraction (Siemens D-5000 Diffractometer, using a Cu K_α radiation, 0.15406 nm), under a grazing angle condition for all the films. The surface morphology of the films was got in a Scanning Electron Microscope (Jeol, JSM-6390LV). The chemical composition of the films was obtained in an Inca x-sight Oxford Instruments characteristic X-ray microanalysis system (EDS), attached to this microscope. Finally, an LSE Stokes (Gaertner Scientific Corporation) single wavelength ellipsometer (6328 Å, He-Ne laser measuring beam at a 70° incidence angle) was used to get the index of refraction of the films. Up to five different sites on top of the films surface ($\sim 1 \times 1.5$ cm) were randomly selected to measure the index of refraction by ellipsometry.

3. Results and Discussion

3.1. Scanning Electron Microscopy and Energy Dispersive Spectroscopy

The films as deposited were analyzed by EDS. The elemental composition of Cd, Zn and O was measured in each film and was used to estimate the relative amount of CdO and ZnO. A low voltage acceleration was used in the SEM (10 kV) in order to get a better estimation of the films elemental composition (since some of them resulted thin in thickness, see Table I). Film B, deposited at 300°C presented a $\text{ZnO}_{0.58}\text{-CdO}_{0.42}$ composition, and its equivalent of 400°C (film F), $\text{ZnO}_{0.60}\text{-CdO}_{0.40}$. These films were both deposited with a relative concentration in the spraying solution of 50/50 at% of Zn/Cd. It is observed that the final composition obtained in the films was about 60% and 40% of ZnO and CdO, respectively. Films C and G, deposited with 75/25 at% of Zn/Cd resulted with a composition of $\text{ZnO}_{0.71}\text{-CdO}_{0.29}$ and $\text{ZnO}_{0.78}\text{-CdO}_{0.22}$, respectively, (deposited at 300°C and 400°C, respectively). For the latter films the spraying solutions were proposed to be 75 at% Zn and 25 at% Cd, from their respective reagents. In this latter case, the final composition in the films resulted closer to the proposed one. The results of the composition of the films are listed in Table I. Figure 1 shows some images of the surface morphology of the different

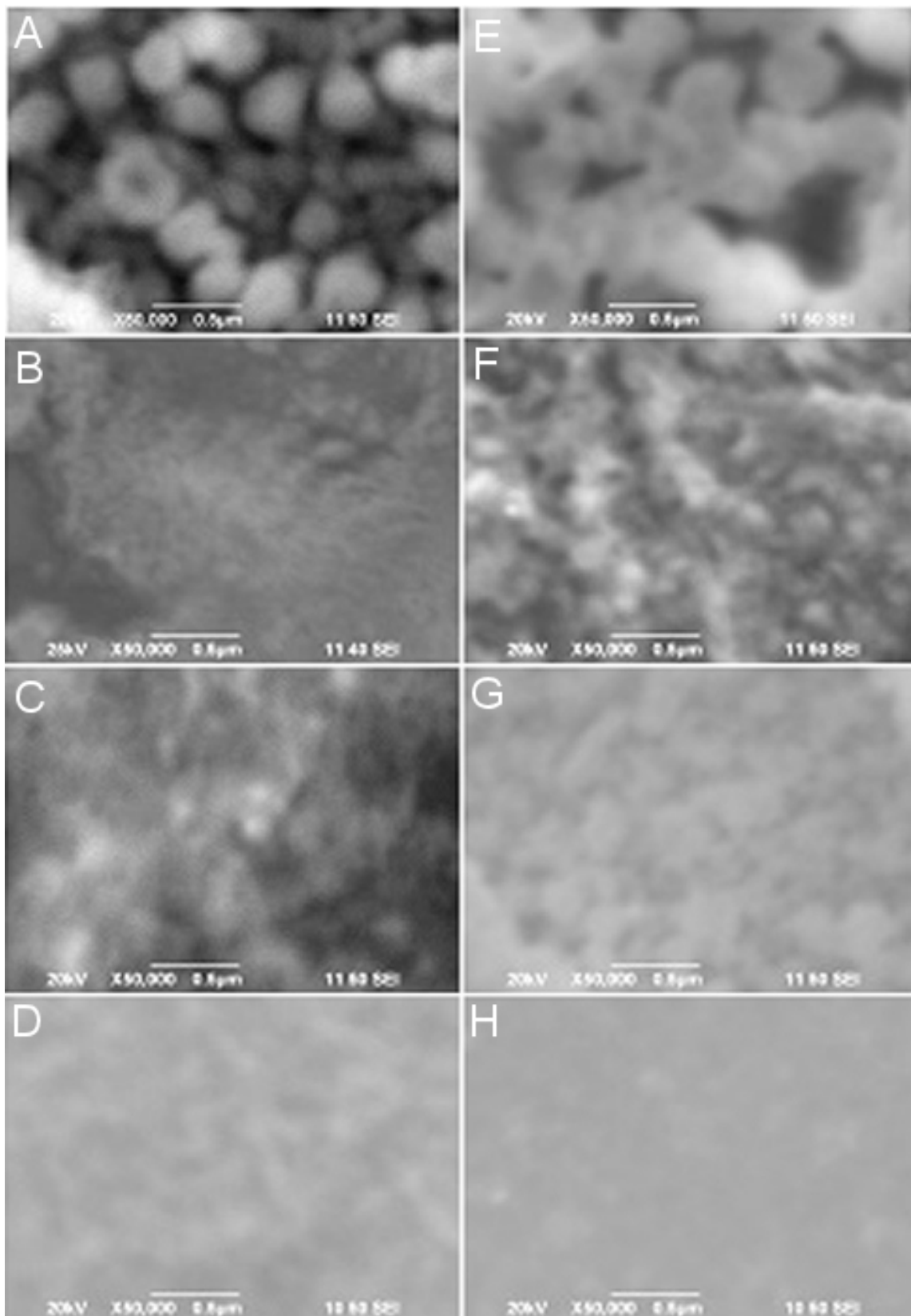


FIGURE 1. Surface morphology of the $(\text{ZnO})_x(\text{CdO})_{1-x}$ films. Image A ($X = 0$, deposited at 300°C), B ($X = 0.58$, deposited at 300°C), C ($X = 0.71$, deposited at 300°C), D ($X = 1$, deposited at 300°C), E ($X = 0$, deposited at 400°C), F ($X = 0.6$, deposited at 400°C), G ($X = 0.78$, deposited at 400°C), and H ($X = 1$, deposited at 300°C).

TABLE I. Structural and electrical characteristics of $(\text{CdO})_X-(\text{ZnO})_{1-X}$ thin films.

Film	Composition in spray solution	Composition obtained in the films	Thickness (nm)	Impedance Spectroscopy			
				Equivalent circuit used to fit films B, D, F, G and H.			
				R1(Ω)	C1(F)	R2 (Ω)	Origin
Equivalent circuit to fit film C.							
Deposition temperature (300°C)							
A	100 at% Cd/ 0 at% Zn	CdO	430				
B	50 at% Cd/ 50 at% Zn	$(\text{ZnO})_{0.58}(\text{CdO})_{0.42}$	190	83.9	1.98×10^{-9}	313	Grain boundary
C	25 at% Cd/ 75 at% Zn	$(\text{ZnO})_{0.71}(\text{CdO})_{0.29}$	135	2967	8.59×10^{-12}		Bulk (grain)
				1767	4.64×10^{-10}	162	Grain boundary
D	0 at% Cd/ 100 at% Zn	ZnO	100	13.4×10^6	7.05×10^{-12}	1199	Bulk (grain)
Deposition temperature (400°C)							
E	100 at% Cd/ 0 at% Zn	CdO	180				
F	50 at% Cd/ 50 at% Zn	$(\text{ZnO})_{0.60}(\text{CdO})_{0.40}$	120	542.3	1.60×10^{-11}	346	Grain boundary
G	25 at% Cd/ 75 at% Zn	$(\text{ZnO})_{0.78}(\text{CdO})_{0.22}$	290	7867	7.68×10^{-12}	88.7	Bulk (grain)
H	0 at% Cd/ 100 at% Zn	ZnO	100	13.4×10^6	7.56×10^{-12}	1271	Bulk (grain)

$(\text{ZnO})_X(\text{CdO})_{1-X}$ films. The surface morphology was imaged at 50000X with an accelerating voltage of 20-25kV. Film A shows a grainy microstructure, where the shape of the grains were approximately spherical. Film E (deposited at 400°C), shows a microstructure of grains that seem to be more interconnected, probably due to the higher substrate temperature during deposition of the films. The surface morphology of film E seems similar to the one reported by Salunkhe et al. for nanocrystalline CdO films obtained by spray pyrolysis using cadmium acetate too [23]. In contrast, films D and H seem to have smaller grains. Films B and F, and films C and G, seem to show intermediate morphologies between those of CdO and ZnO. However, films deposited at 400°C seem to be more grainy (Films F and G), compared with films B and C. Probably, the substrate temperature in-

fluenced dramatically on the microstructure of the films. The chemical composition in films B, C, F and G, indicates that the amount of CdO was larger than 22%, so it is probable the presence of a mixture of phases of CdO and ZnO, as X-ray diffraction results, described in next section, will confirm. P. Misra *et al.* and T. Makino *et al.* [10,11] found out that when the amount of CdO in the films is larger than 8%, a segregation of CdO results in them, instead of obtaining a single CdZnO phase. In our case, obtaining films with mixtures of CdO and ZnO was important in order to have TCO's with high conductivity and transparency. Even though the optical properties (% of transmittance and determination of the band gap) are not shown explicitly in this work, the films resulted with a high transparency and with a band gap ranging from ZnO to CdO.

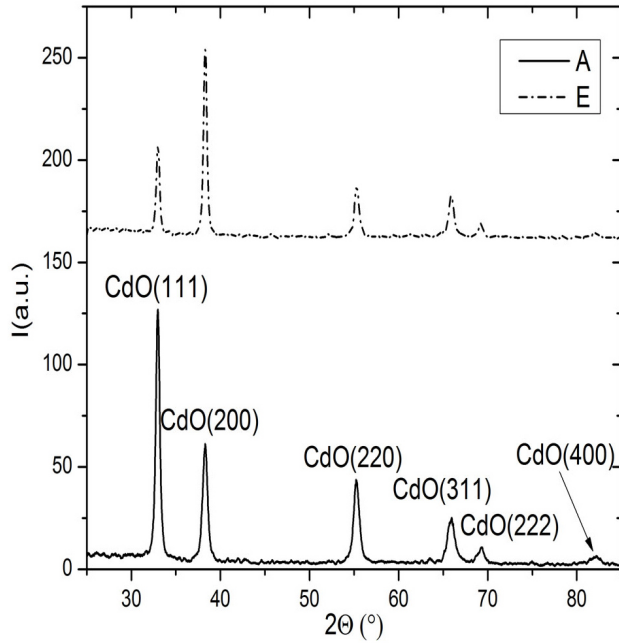


FIGURE 2. X-ray diffraction spectra of films of CdO deposited at 300°C (A), and CdO deposited at 400°C (E).

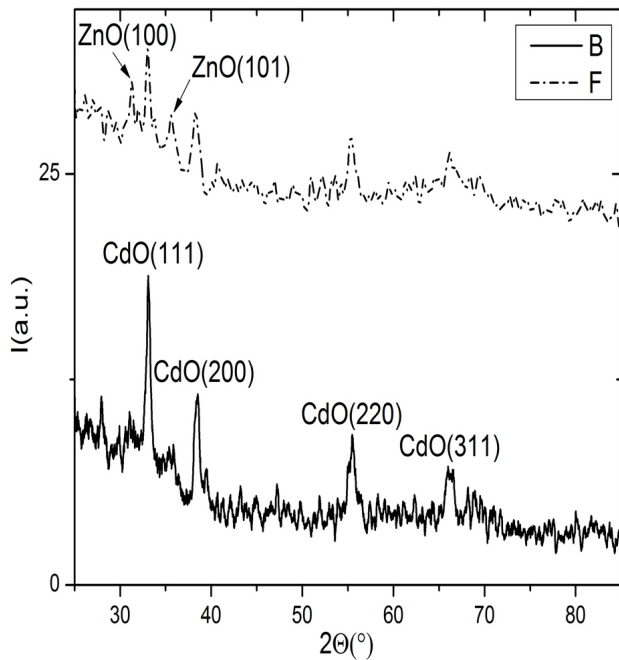


FIGURE 3. X-ray diffraction spectra of films of $(\text{ZnO})_{0.58}(\text{CdO})_{0.42}$ deposited at 300°C (B), and $(\text{ZnO})_{0.60}(\text{CdO})_{0.40}$ deposited at 400°C (F).

3.2. X-ray Diffraction

Figures 2 to 5 show the diffraction patterns of the films deposited. In general, all films were polycrystalline. For example, the diffraction peaks of films A and E, Fig. 2, corresponded to the known cubic rocksalt lattice of the CdO phase (ICDD # 00-073-2245). An interesting feature observed is

that film E showed a preferred (200) orientation, probably because of flatter shaped grains, shown in image E, Fig. 1. The higher substrate temperature could have induced probably the preferred orientation in this film. The crystalline index (C.I.) was calculated in films A and E, and resulted of about 0.97 and 0.91, respectively. This indicates that the polycrystalline

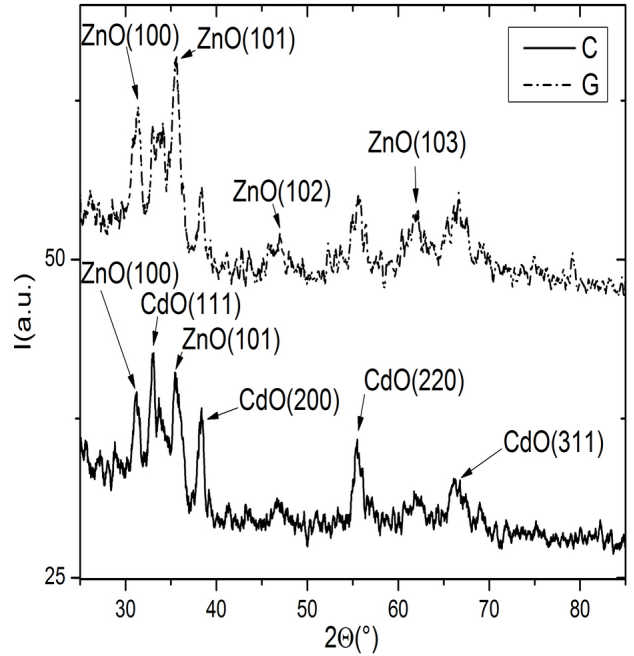


FIGURE 4. X-ray diffraction spectra of films of $(\text{ZnO})_{0.71}(\text{CdO})_{0.29}$ deposited at 300°C (C), and $(\text{ZnO})_{0.78}(\text{CdO})_{0.22}$ deposited at 400°C (G).

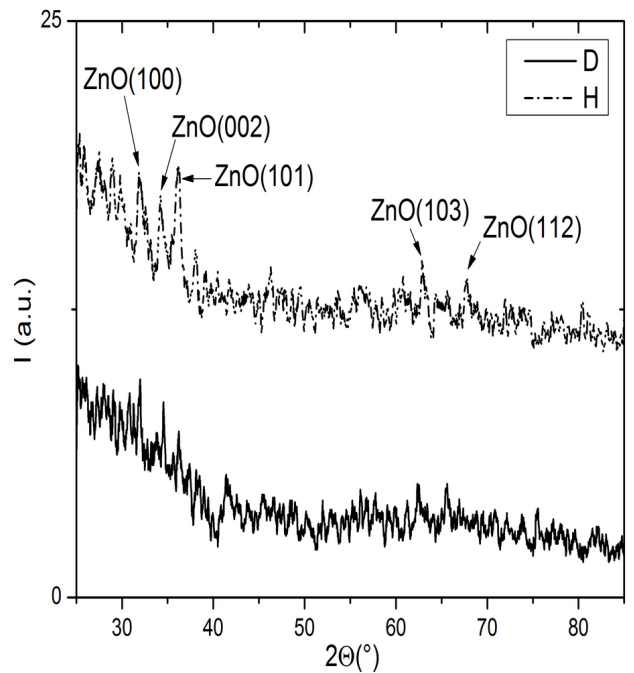


FIGURE 5. X-ray diffraction spectra of films of ZnO deposited at 300°C (D), and ZnO deposited at 400°C (H).

nature of the films was almost the same, or it was a little bit enhanced in the films deposited at the lower temperature (300°C). (Note that the thickness of film E is lower than the thickness of film A, see Table I). Figure 1 shows that the films deposited at 400°C seem to have more defined grains and/or with a larger size in average, indicating that the higher the deposition temperature in the films, the larger the grain size. Most reports have shown the polycrystalline nature of CdO films that are obtained by spray pyrolysis at temperatures in the range of 200-400°C, however, in most of those reports, a post-thermal annealing at 450°C has been necessary to improve their properties [12,14-16]. Figure 3 compares films B and F. The peaks of CdO are clearly seen in film B (film deposited at 300°C), however, the peaks of ZnO are not easily noticed, suggesting that at this temperature the ZnO phase is kind of amorphous and/or the ZnO grain size is too small to be noticed in the diffraction patterns. In contrast, film F seems to show some of the diffraction peaks of both CdO and ZnO. This fact indicates that a higher temperature is needed to improve the polycrystalline nature in ZnO. In general, under certain conditions, a mixture of phases has been found in this type of films [12,14-16]. Figure 4 compares films C and G. In this case, for the film deposited at 300°C (film C), a clearer participation of both phases (CdO and ZnO) is obtained. The same approximation can be said for the films deposited at 400°C (film G). It is probable that because of the larger amount of Zn in solution, the ZnO phase is more noticed. Finally, Fig. 5 shows the diffraction patterns of the films of ZnO deposited at 300°C and 400°C (films D and H). In this case, the film H shows more clearly the ZnO peaks. It is observed that for ZnO, the higher the substrate tempera-

ture, the more polycrystalline film. ZnO films resulted in all cases with the known hexagonal wurtzite structure (JCPDS-ICDD # 36-1451).

3.3. Ellipsometry

The results of X-ray diffraction and SEM-EDS seem to be confirmed by the results of the index of refraction of the films, as determined by ellipsometry. The behavior of the index of refraction is shown in Fig. 6. Film A showed the highest index of refraction (close to 2.1), suggesting that film A was denser (crystalline CdO shows an index of refraction of ~2.49 [24]). This can probably be inferred from Fig. 1E, since we can notice more empty spaces in film E. The latter conclusion about the correlation between the specific density of the film and its index of refraction has been applied to other type of thin films, such as silicon dioxide or aluminum oxide [25,26]. This also seems to be in agreement with the X-ray diffraction pattern (Fig. 2), since the crystalline index is a little bit higher in film A than in film E, deposited at 300°C and 400°C, respectively. Films B and C show a higher index of refraction compared to films F and G, probably because the content of CdO is larger in the primer than in the latter set of films, and/or because of the grainy nature with more empty space in films deposited at 400°C than at 300 °C. In the extreme case (for ZnO, films D and H), deposited at 300°C and 400°C, respectively, the index of refraction (1.819) in film H is larger because at this temperature the polycrystalline nature

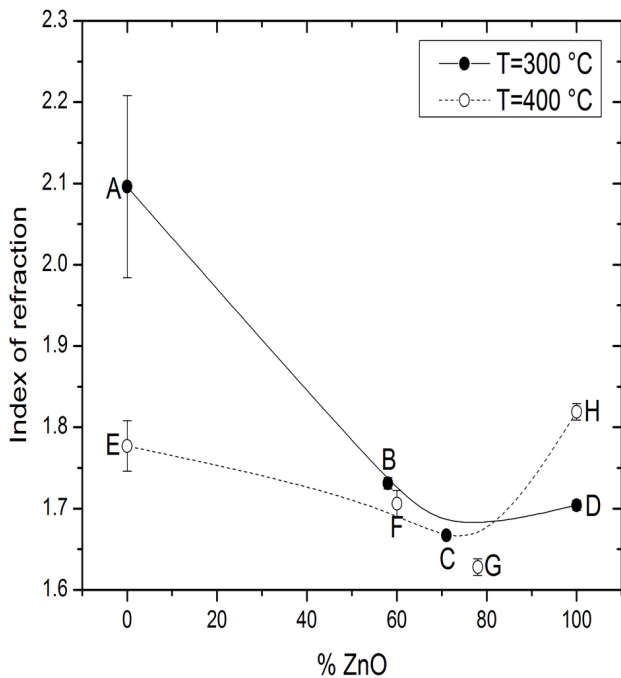


FIGURE 6. Index of refraction of the $(ZnO)_x(CdO)_{1-x}$ films as a function of the % ZnO content.

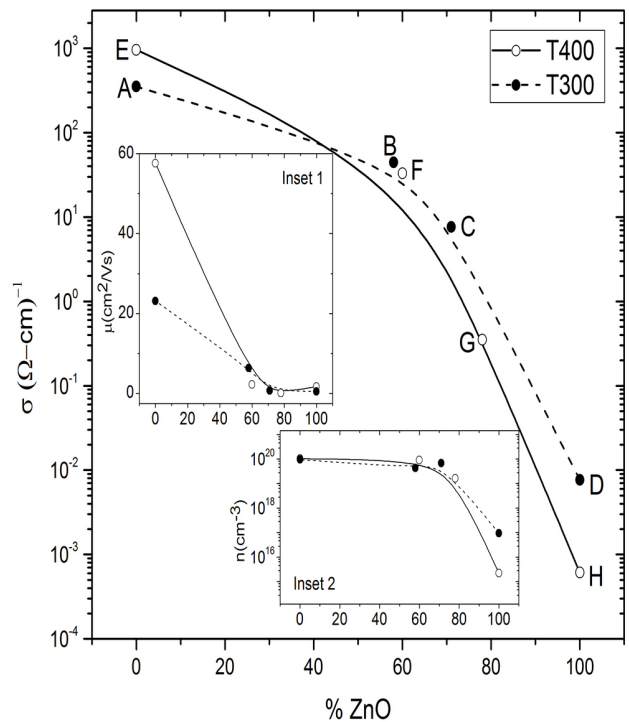


FIGURE 7. Electrical conductivity of the $(ZnO)_x(CdO)_{1-x}$ films as a function of the % ZnO content. Inset 1 shows the mobility and Inset 2 shows the carrier concentration, as a function of the % ZnO content.

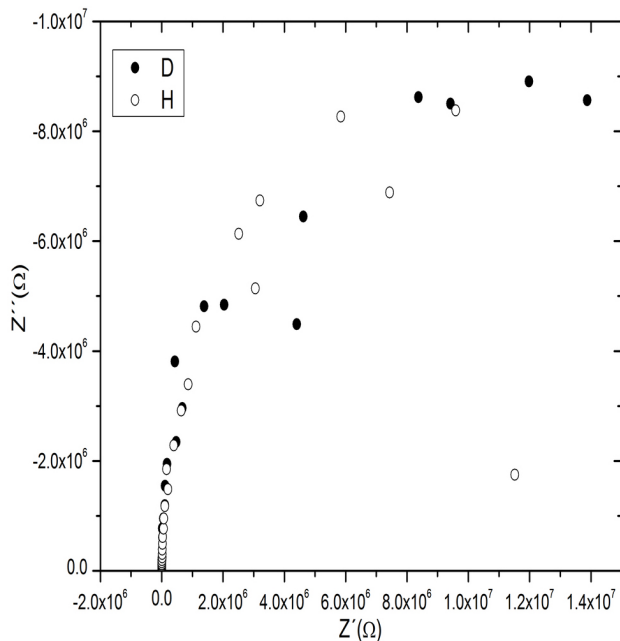


FIGURE 8. Impedance data for films of ZnO deposited at 300°C (D), and ZnO deposited at 400°C (H), presented in the complex impedance format.

of ZnO resulted enhanced, as compared to the polycrystalline nature of film D (with an index of refraction of 1.70). Crystalline ZnO shows an index of refraction of ~ 2.00 [24]. In fact, film D resulted kind of amorphous, suggesting probably a lower index of refraction in it.

3.4. Electrical Properties

Figure 7 and its insets 1 and 2 show the electrical properties of the films as determined by Hall Effect measurements. All the $(\text{ZnO})_X(\text{CdO})_{1-X}$ films resulted in n-type conductivity. It can be observed that their conductivity was found approximately in the range of $\sim 1 \times 10^3$ to $\sim 6 \times 10^{-4} (\Omega\text{-cm})^{-1}$, depending on the relative amount of CdO in the films. It is important to notice that this conductivity was measured in the as deposited films, without any further post-thermal annealing in reducing atmospheres. Specifically, film E showed a conductivity of $9.6 \times 10^2 (\Omega\text{-cm})^{-1}$, whereas in film A the conductivity was about $3.5 \times 10^2 (\Omega\text{-cm})^{-1}$. Taking into account the relationship for the electrical conductivity, [27] (where is electrical conductivity, is the carrier mobility, the carrier concentration, and the electronic charge), the enhanced conductivity in film E is probably attributed to the higher mobility of carriers (see inset 1), since both type of films show almost the same carrier density (see inset 2). The higher mobility in film E might be due to a more interconnected microstructure and/or to a larger grain size microstructure in the films, as can be inferred from Fig. 1. The high value of the conductivity in CdO films is characteristic in them, and it has been attributed to the relatively large concentration of ionized atomic defects, such as oxygen vacancies or cadmium interstitials [6]. On the other hand, the ZnO films (films D and H) showed a conduc-

tivity as low as $6.1 \times 10^{-4} (\Omega\text{-cm})^{-1}$, (film H, deposited at 400°C). Intrinsic ZnO thin films show in general a high resistivity (or a low conductivity), when deposited by many of the conventional deposition techniques [2]. A more insulating ZnO film was obtained in film H than in film D probably because of the lower carrier concentration (see inset 2). For the rest of the films (films B, C, F and G), it can be observed that the films deposited at 300°C show in average a higher conductivity, probably due to the larger amount of the CdO phase in them. So, the CdO phase seems to play an important role in the electrical measurements, since its presence seems to limit, in average, the electrical behavior in the films. The polycrystalline nature, as well as the microstructure of the films could also play a key role in the electrical behavior of the mixture of high and low conducting phases. It is thought that the different proportions and/or distributions of phases are an interesting issue to be studied. In polycrystalline solids, transport properties are strongly affected by their microstructure, and impedance spectra usually contain features that can be related to them [28]. A study by impedance spectroscopy was done in all of the films (Figs. 8 to 10), except for the set of CdO films, since they were highly conductive. In the case of ZnO (films D and H), the complex impedance spectra (Nyquist diagram) shows the presence of one time constant (indicated by one fair semi-circle arc), Fig. 8. Since only one time constant was suggested in the diagram, the experimental data was fitted by an equivalent circuit consisting of a parallel RC circuit in series with a resistor (using the Z-VIEW software). The equivalent circuit is shown in Table I. In film H, the fitting results were $R1g \sim 13.4 \text{ M}\Omega$, and $C1g \sim 7.56 \text{ pF}$, and in film D, $R1g \sim 13.1 \text{ M}\Omega$ and $C1g \sim 7.05 \text{ pF}$. The fitting results are tabulated in Table I. These results seem to be in agreement with the Hall Effect measurements, Fig. 7, since film H shows a lower conductivity (a higher resistivity) than film D. The resistance R2, listed in Table I, can be attributed to the silver paint electrodes and wiring resistances associated with the measurement. Since the capacitance in both cases was in the range of pF, the origin of this time constant is due very probably to the grains (bulk) of ZnO in the films [29]. Impedance spectroscopy of ZnO films, deposited by spray pyrolysis, has been studied by R. Martins et al. when studying ZnO as an ozone sensor, [30]. CdO and ZnO single films constitute conducting and insulating phases, respectively, and it is important to study what occurs when a mixture of both phases is present in a single film. Figure 9 compares films C and G. Film G, deposited at 400°C, shows clearly one time constant in the Nyquist diagram. Applying the same equivalent circuit for fitting the semi-circle arc we obtained $R1g \sim 7867 \Omega$ and $C1g \sim 7.68 \text{ pF}$. The capacitance value for this time constant suggest very probably that also in this case the grains are responsible for this response. In contrast, film C, deposited at 300°C, depicts clearly two time constants (indicated by two well-resolved semi-circle arcs). The equivalent circuit for fitting the Nyquist diagram for film C consisted of the series of two parallel RC circuits and a single resistor in series (the circuit is shown in Table I). The first semi-circle

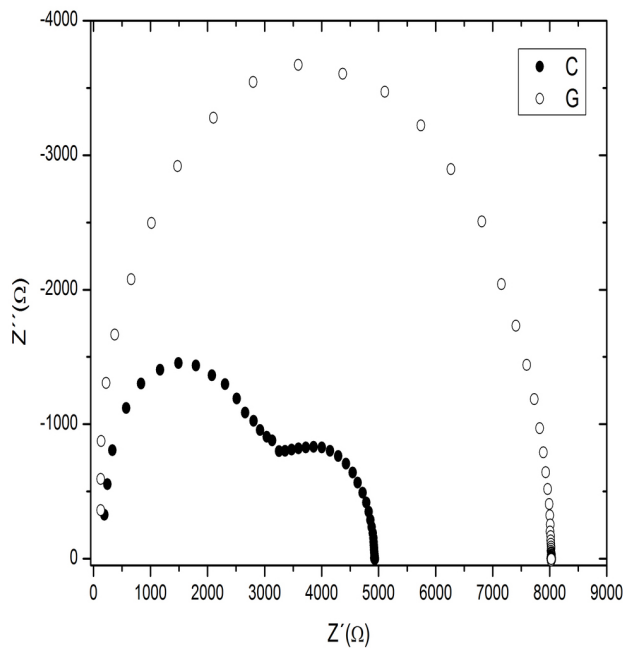


FIGURE 9. Impedance data for films of $(\text{ZnO})_{0.71}(\text{CdO})_{0.29}$ deposited at 300°C (C), and $(\text{ZnO})_{0.78}(\text{CdO})_{0.22}$ deposited at 400°C (G), presented in the complex impedance format.

(high frequency) showed a resistance R_{1g} of about 2967Ω , and a capacitance C_{1b} of about 8.59 pF , and in the second semi-circle (lower frequency), the resistance R_{1gb} was about 1767Ω , and a capacitance C_{1gb} of about $4.64 \times 10^{-10} \text{ F}$. The resistance R_2 was about 160Ω . The time constant of the second semi-circle might indicate that the response is due to grain boundaries [29]. The total effect of mixing conducting and insulating phases in a single film is that in average the resistance (or the resistivity) of the whole film is decreased, caused by the distribution and/or concentration of the high conducting phase(s) [31]. In case of film G, even though it can't be noticed a second semi-circle arc, due to grain boundaries (the reason is not clear in this moment), the resistivity of the whole film is reduced too. In the case of films B and F, Fig. 10, film F shows also one time constant where $R_{1gb} \sim 542 \Omega$, and $C_{1gb} \sim 1.6 \times 10^{-11} \text{ F}$. Because of the time constant, the response might be due to grain boundaries, and again, the higher the concentration of CdO in the film (40 %), the lower the resistivity of the whole film. In film B, containing 42 % of CdO, the resistivity of the whole film (83.9Ω) was further reduced, and the value of the capacitance (about $2 \times 10^{-9} \text{ F}$), indicated a grain boundary response in this film too. These experimental results led us to think that in the $(\text{ZnO})_X(\text{CdO})_{1-X}$ system, the highly conducting character of CdO influenced dramatically the conductivity of the films. Its influence depends strongly on its relative amount and also on the deposition temperature. Both, the bulk or grains, as well as the grain boundaries limit the electrical properties in the $(\text{ZnO})_X(\text{CdO})_{1-X}$ mixture.

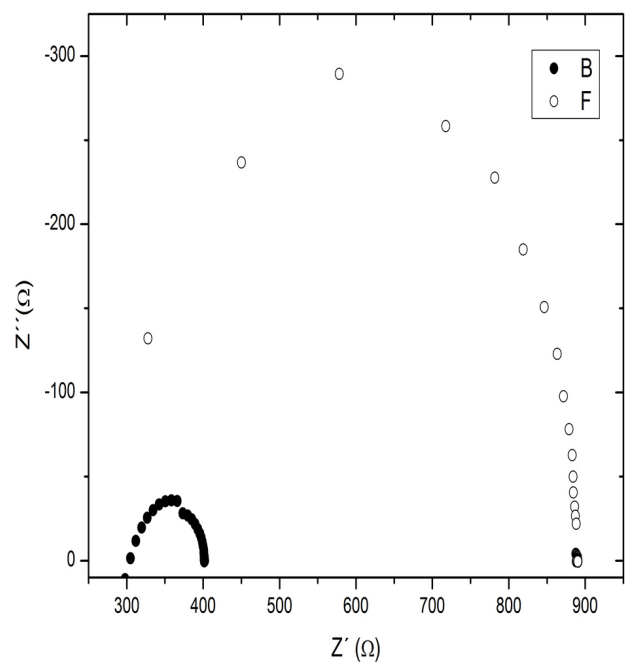


FIGURE 10. Impedance data for films of $(\text{ZnO})_{0.58}(\text{CdO})_{0.42}$ deposited at 300°C (B), and $(\text{ZnO})_{0.60}(\text{CdO})_{0.40}$ deposited at 400°C (F), presented in the complex impedance format.

4. Conclusions

Polycrystalline and dense $(\text{ZnO})_X(\text{CdO})_{1-X}$ thin films were obtained by the cheap ultrasonic spray pyrolysis technique at 300°C and 400°C from cadmium and zinc acetates. The composition of the films was varied between that of CdO, the highly conducting phase, and that of ZnO, the highly insulating film. The conductivity of the CdO phase was close to $1 \times 10^3 (\Omega\text{-cm})^{-1}$, the highest value reported for non-doped CdO films, without any post-thermal treatment annealing. The index of refraction of the films confirmed the structural studies carried out by X-ray diffraction and scanning electron microscopy, as well as the energy dispersive spectroscopy results. Impedance spectroscopy confirmed the results got by Hall Effect and showed that the highly conducting character of CdO influenced dramatically the conductivity of the films. Its influence depended strongly on its relative amount and also on the deposition temperature. Both, the bulk or grains, as well as the grain boundaries limit the electrical properties in the $(\text{ZnO})_X(\text{CdO})_{1-X}$ mixture system.

Acknowledgements

The authors would like to acknowledge the financial support from Conacyt-Mexico project CB-2009/129227 and SIP-IPN projects 20101556, 20111101, 20121458 and Multidisciplinary Project # 1558 (2013). The PIFI-IPN program is also acknowledged. The technical support from M. Guerrero, Alfonso Martinez, and Z. Rivera is also recognized.

1. D.S. Ginley and J.D. Perkins, in: D.S. Ginley, D.C. Paine (Eds.), *Handbook of Transparent Conductors*, (Springer, New York, 2010), pp. 1.
2. H.L. Hartnagel, A. L. Dawar, A.K. Jain, C. Jagadish, *Semiconducting Transparent Thin Films*, Institute of Physics Publishing, (Institute of Physics, London, 1995).
3. A.J. Freeman, K.R. Poeppelmeier, T.O. Mason, R.P.H. Chang, T.J. Marks, MRS BULLETIN/August (2000) 45.
4. Ü. Özgür, Y.I. Alivov, C. Liu, A. Teke, M.A. Reshchikov, S. Doan, V. Avrutin, S.-J. Cho, H. Morkoç, *J. Appl. Phys.* **98** (2005) 041301.
5. P. Barquinha, R. Martins, L. Pereira, E. Fortunato, *Transparent Oxide Electronics From Materials to Devices*, (J. Wiley & Sons, Ltd. Singapore, 2012).
6. F.P. Koffyberg, *Canadian Journal of Physics* **49** (1971) 435.
7. Z.Y. Zhao, D.L. Morel, C.S. Ferekides, *Thin Solid Films* **413** (2002) 203.
8. B.J. Zheng, J.S. Lian, L. Zhao, and Q. Jiang, *Appl. Surf. Sci.* **256** (2010) 2910.
9. S. Sadofev, P. Schäfer, Y.-H. Fan, S. Blumstengel, F. Henneberger, D. Schulz, and D. Klimm, *Appl. Phys. Lett.* **91** (2007) 201923.
10. P. Misra, P.K. Sahoo, P. Tripathi, V.N. Kulkarni, R.V. Nandedkar, and L.M. Kukreja, *Appl. Phys. A* **78** (2004) 37.
11. T. Makino, Y. Segawa, M. Kawasaki, A. Ohtomo, R. Shiroki, K. Tamura, T. Yasuda, and H. Koinuma, *Appl. Phys. Lett.* **78** (2001) 1237.
12. A.S. Aybek, N. Baysal, M. Zor, E. Turan, and M. Kul, *Thin Solid Films* **515** (2007) 8709.
13. R. Ferro, J.A. Rodriguez, I. Jiménez, A. Cirera, J. Cerdà, and J.R. Morante, *IEEE SENSORS JOURNAL* **5** (2005) 48.
14. O. Vigil, L. Vaillant, F. Cruz, G. Santana, A. Morales-Acevedo, and G. Contreras-Puente, *Thin Solid Films* **361** (2000) 53.
15. G. Santana, A. Morales-Acevedo, O. Vigil, L. Vaillant, F. Cruz, and G. Contreras-Puente, *Thin Solid Films* **373** (2000) 235.
16. O. Vigil, F. Cruz, G. Santana, L. Vaillant, A. Morales-Acevedo, and G. Contreras-Puente, *Appl. Surf. Sci.* **161** (2000) 27.
17. S. Vijayalakshmi, S. Venkataraj, and R. Jayavel, *J. Phys. D.: Appl. Phys.* **41** (2008) 245403.
18. Z. Bi-Ju, L. Jian-She, Z. Lei, and J. Qing, *Chin. Phys. Lett.* **28** (2011) 016801.
19. G. Blandenet, M. Court, and Y. Lagarde, *Thin Solid Films* **77** (1981) 81.
20. L. Martinez Pérez, M. Aguilar-Frutis, O. Zelaya-Angel, and N. Muñoz-Aguirre, *Phys. Stat. Sol. (a)* **203** (2006) 2411.
21. L.L. Diaz-Flores, R. Ramirez-Bon, A. Mendoza-Galván, and E. Prokhorov, *Journal of Physics and Chemistry of Solids* **64** (2003) 1037.
22. O.K. Varghese and L.K. Malhotra, *J. Appl. Phys.* **87** (2000) 7457.
23. R.R. Salunkhe, D.S. Dhawale, D.P. Dubal, C.D. Lokhande, *Sensors and Actuators B* **140** (2009) 86.
24. R.C. Weast (Ed), *Handbook of Chemistry and Physics*, 50th edition, (The Chemical Rubber Co. 1969).
25. W.A. Pliskin and H.S. Lehman, *J. of the Electrochem. Soc.* **112** (1965) 1013.
26. M. Aguilar-Frutis, M. Garcia, and C. Falcony, *Appl. Phys. Lett.* **72** (1998) 1700.
27. M. A. Omar, *Elementary Solid State Physics*, (Addison-Wesley Publishing Company Inc., Philippines, 1975).
28. N. Bonanos, B.C.H. Steele, and E.P. Butler, in: E. Barsoukov, J.R. Macdonald (Eds.), *Impedance Spectroscopy Theory, Experiment, and Applications*, (John Wiley & Sons, Inc. Hoboken, New Jersey, Second Edition, 2005). pp. 205.
29. J.T.S. Irvine, D.C. Sinclair, and A.R. West, *Adv. Mater.* **2** (1990) 132.
30. R. Martins E. Fortunato, P. Nunes, I. Ferreira, A. Marqués, M. Bender, N. Katsarakis, V. Cimalla, G. Kiriakidis, *J. Appl. Phys.* **96** (2004) 1398.
31. V.F. Lvovich, *Impedance Spectroscopy, Applications to Electrochemical and Dielectric Phenomena*, (J. Wiley & Sons, Inc., Hoboken, New Jersey, 2012).